


# Comparability of radar and optical methods in identifying surface water in a semi-arid protected area

Zorodzai Dzinotizei<sup>1,2</sup> | Hilton G. T. Ndagurwa<sup>2,3</sup>  | Henry Ndaimani<sup>4</sup>  | Angella Chichinye<sup>1</sup>

<sup>1</sup>Department of Forest Resources and Wildlife Management, Faculty of Environmental Science, National University of Science and Technology, Bulawayo, Zimbabwe

<sup>2</sup>Department of Geospatial Science, Faculty of Environmental Science, National University of Science and Technology, Bulawayo, Zimbabwe

<sup>3</sup>School of Animal, Plant and Environmental Sciences, University of the Witwatersrand, Johannesburg, South Africa

<sup>4</sup>Department of Geography and Environmental Science, Faculty of Science, University of Zimbabwe, Harare, Zimbabwe

## Correspondence

Zorodzai Dzinotizei, Department of GeoForest Resources and Wildlife Management, Faculty of Environmental Science, National University of Science and Technology, PO Box AC 939 Ascot, Bulawayo, Zimbabwe.

Email: [zorodzai.dzinotizei@nust.ac.zw](mailto:zorodzai.dzinotizei@nust.ac.zw)

## Abstract

Surface water assumes a pivotal role in sustaining a wide range of wildlife species in semi-arid protected areas. However, differences in surface water body typology, underlying soil type, wildlife activity, the presence of phytoplankton amongst other factors, result in high variability of surface water spectral reflectance and detection accuracy. In this study, the performance of radar and optical methods was evaluated in detecting surface water of variable spectral reflectance in Hwange National Park, Zimbabwe using Sentinel-1 radar and Sentinel-2 optical images for the period 2016–2023. Results demonstrated that radar methods had low surface water detection accuracy which was highly variable as shown by overall accuracy and kappa statistic measures which continuously changed over time compared with optical methods. The overall best-performing method was the optical  $AWEI_{nsh}$  (sharpened) which showed high surface water detection accuracy and consistency (OA: 94%–100%) and ( $\kappa$ : 0.88–1.00) from 2016 to 2023. Therefore, optical methods present a stable and robust way for surface water monitoring in heterogeneous semi-arid protected areas. However, radar-based methods should be continually explored where optical-based technologies are impeded as a result of vegetation cover and cloud conditions.

## KEYWORDS

climate change, Hwange National Park, remote sensing, surface water bodies

## Résumé

Les eaux de surface jouent un rôle essentiel dans le maintien d'un nombre important d'espèces sauvages vivant dans les zones protégées semi-arides. Cependant, les différences dans la typologie des masses d'eau de surface, le type de sol sous-jacent, l'activité de la faune, la présence de phytoplancton, entre autres facteurs, entraînent une grande variabilité de la réflectance spectrale de l'eau de surface et de la précision de la détection. Dans cette étude, la performance des méthodes radar et optiques a été évaluée pour la détection des eaux de surface de réflectance spectrale variable dans le parc national de Hwange, au Zimbabwe, en utilisant les images radar Sentinel-1 et les images optiques Sentinel-2 pour la période 2016–2023. Les résultats ont démontré que les méthodes radar offraient un faible niveau de précision de détection des eaux de surface, qui était très variable, comme l'illustrent les mesures de précision globale et de statistique kappa qui ont continuellement changé au fil du temps par rapport

aux méthodes optiques. La méthode la plus performante était la méthode optique AWEI<sub>nsh</sub> (sharpened) qui a offert un niveau de précision élevé et constant dans la détection des eaux de surface (OA : 94 %-100 %) et ( $\kappa$  : 0,88-1,00) de 2016 à 2023. Par conséquent, les méthodes optiques constituent un moyen stable et efficace pour la surveillance des eaux de surface dans les zones protégées semi-arides hétérogènes. Cependant, les méthodes basées sur le radar devraient continuer à être explorées lorsque les performances des technologies basées sur l'optique sont compromises en raison de la couverture végétale et des conditions nuageuses.

## 1 | INTRODUCTION

Surface water availability influences the diversity, distribution, and interactions of wildlife in semi-arid protected areas (Bartzke et al., 2018; Chamailé-Jammes et al., 2007). Due to the ephemeral nature of natural surface water bodies in semi-arid protected areas, artificial water sources (e.g., boreholes) augment game water supply, particularly during the dry season (Gaylard et al., 2003). However, supplementary surface water provision is associated with several ecological issues. For example, excessive water points favour water-dependent ungulates and elephants, increase vegetation damage, reduce the spatio-temporal heterogeneity of habitats, amongst many others (Davidson et al., 2013; Owen-Smith, 1996; Smit et al., 2007). Therefore, regular monitoring of surface water availability is essential to better inform both surface water provision and wildlife habitat management policies, especially in water-limited ecosystems.

In the late dry season, both aerial and ground monitoring surveys have been employed to monitor surface water availability, but these are time and resource-intensive (Kaplan & Avdan, 2017). This limits the area covered and reduces monitoring frequency. Remote sensing which uses freely available satellite imagery enables surface water detection at large spatial scales and high temporal intervals (Senay et al., 2013). However, remote sensing is sensitive to variations in properties of surface water bodies (Li et al., 2022). Surface water bodies vary in typology, perimeter, depth, underlying soil type, and intensity of use by wildlife. These factors affect surface water depth, suspended particulate matter, the concentration of nutrients, amount of cyanobacteria, phytoplankton, and aquatic macrophytes influencing the spectral signature of surface water (Gupta, 2017; Rotkiske & Bostater Jr, 2018). For example, phytoplankton biomass has high-spectral reflectance in the near-infrared region of the electromagnetic spectrum and in contrast, clear water has low spectral reflectance in this region (Kutser, 2009). Such variations in surface water body properties result in high variability of surface water spectral reflectance and detection accuracy. Thus, to ensure accurate detection of surface water, remote sensing-based methods which are robust to these spectral complexities should be applied.

Most studies for extracting surface water information have been based on optical sensors due to free access to data and historical data archives (Bhangale et al., 2020; Mishra et al., 2020). The launch into space of Sentinel-1 satellite has made radar data freely available at high spatial and temporal configurations (Slagter et al., 2020). The advantage of the Sentinel-1 radar sensor is that it is not impeded by cloud cover and the

radar signal can penetrate through tree canopy gaps due to its longer wavelength (Huang et al., 2017; Slagter et al., 2020) whereas Sentinel-2 optical sensor becomes limited in detecting surface water under dense vegetation cover and cloudy conditions (Peña-Luque et al., 2021).

Radar imagery has successfully been used in flood mapping (Clement et al., 2018), wetland mapping (Behnamian et al., 2017), soil moisture content estimation (Gangat et al., 2020), rice fields mapping (Ovakoglou et al., 2021), and monitoring lake dynamics in different catchments (Zeng et al., 2017). Markert et al. (2018) tested the capability of radar and optical data for mapping surface water by combining the two sensor datasets and applying a water extraction technique to both datasets and produced consistent, harmonised surface water time series information. While radar-based methods are still few and being developed, their ability to detect surface water bodies of variable spectral reflectance in semi-arid ecosystems along with other conventional optical methods, remains under-tested.

The objective of this study was to assess the performance and comparability of radar and optical methods in detecting surface water of variable spectral reflectance in Hwange National Park (HNP), a semi-arid protected area in southern Africa. The study also explored thresholding methods which could improve the performance of radar and optical methods. We expected the performance of Sentinel-1 radar methods to be comparable to that of Sentinel-2 optical methods because of Sentinel-1 sensor's sensitivity to surface water in a range of catchments and high penetrative capacity of radar signal through tree canopy cover. Comparability of radar and optical Sentinel-based methods could allow regular monitoring of surface water availability in heterogeneous semi-arid protected areas under conditions of cloud cover.

## 2 | MATERIALS AND METHODS

### 2.1 | Study area

The study was carried out in HNP which spans an area of 14,651 km<sup>2</sup>. HNP is located in northwest Zimbabwe between latitudes 18°30' and 19°50'S and longitudes 25°24' and 27°24' E (Figure 1). Rainfall ranges between 300 and 800 mm annually which is received mostly between November and April. The northern and North-western portions of the park are drained by the Deka, Lukosi, and Inyantue rivers, tributaries of the perennial

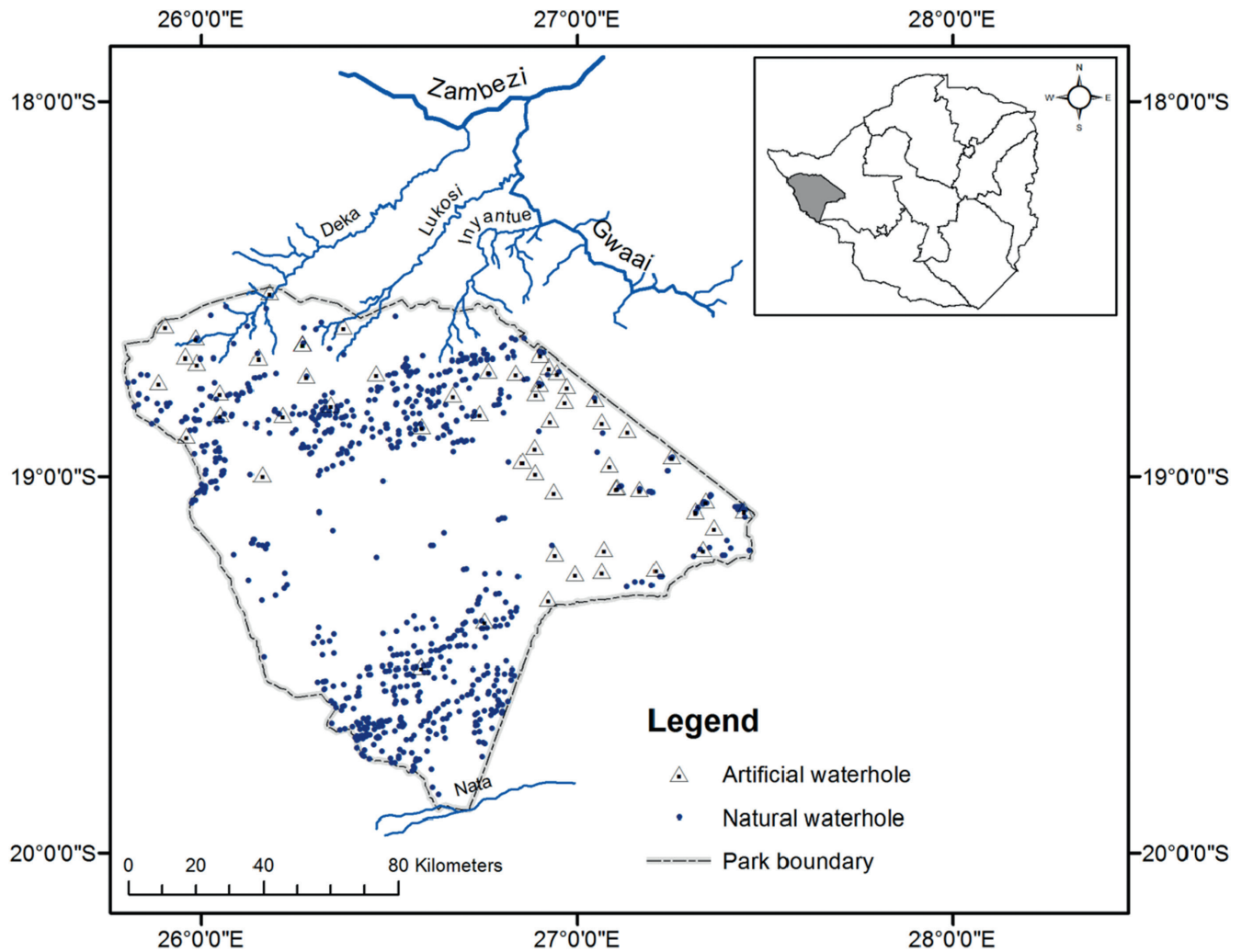


FIGURE 1 Map of Hwange National Park showing different surface water features.

Gwaai river, while the extreme south of the park is drained by Nata river (Rogers, 1993). The river network is seasonal and dries out as the dry season progresses leaving some disconnected river pools (Owen-Smith, 1996). There are diverse surface water body types: artificial waterholes, dams, springs, pans, and small depressions capable of holding water in the wet season.

## 2.2 | Acquisition of remote sensing data

### 2.2.1 | Acquisition and processing of Sentinel-1 data

Sentinel-1 radar images which cover the study area were downloaded from Copernicus Open Access Hub (<https://scihub.copernicus.eu/dhus/#/home>). The Sentinel-1 radar images were for September/October for the years 2016, 2017, 2018, 2019, 2020, 2021, and 2023. Due to the unavailability of Sentinel-1 images for the year 2022 over the study area, we used Sentinel-1 images available for the earliest date, that is, February 2023. The downloaded ground range detected (GRD) imagery in Interferometric Wide (IW) acquisition mode has a pixel spacing of 10m. The Sentinel-1 GRD images were pre-processed in SNAP (Sentinel Applications Platform)

software version 8.0.0 by applying the orbit file, border noise removal, radiometric calibration, terrain correction, and converting the final product to decibel (db) units (Filippini, 2019).

### 2.2.2 | Acquisition and processing of Sentinel-2 data

Sentinel-2 optical images covering the study area were acquired for September/October 2016–2021 and February/March 2023. Sentinel-2 optical images were acquired as Level-1C products and Level-2A products. Level-2A products had undergone geometric, radiometric, and atmospheric corrections from Copernicus Open Access Hub (<https://scihub.copernicus.eu/dhus/#/home>). Level-1C products were processed into Level-2A products using the Sen2Cor version 2.05.05 software (ESA, 2020).

## 2.3 | Water detecting methods

Table 1 shows radar and optical water detecting methods computed in this study.  $AWEI_{nsh}$  and MNDWI (defined in Table 1) were

TABLE 1 Radar and optical methods computed.

Sensor type	Water detecting method	Equation	Reference
Sentinel-1	Vertical-horizontal (VH)	$\lambda VH$	Kim and van Zyl (2009)
	Vertical-vertical (VV)	$\lambda VV$	Kim and van Zyl (2009)
	Polarised Ratio Index (VHrVV)	$\frac{VH}{VV}$	Brisco (2015)
	Normalised Difference Polarisation Index (NDPI)	$\frac{VV - VH}{VV + VH}$	Mitchard et al. (2012)
	Sentinel-1 Water Index (SWI)	$0.1747 \times VV + 0.0082 \times VH \times VV + 0.0023 \times VV^2 - 0.0015 \times VH^2 + 0.1904$	Tian et al. (2017)
	Modified Sentinel-1 Water Index (MSWI)	$0.00045 \times VH - 0.027687 \times (VH - VV) - 0.00429 \times VV \times VH + 0.00489 \times VV^2 - 0.00147 \times VH^2 - 0.92412$	Wang et al. (2019)
Sentinel-2	Automated Water Extraction Index (AWEInsh)	$4 \times (\text{Green} - \text{SWIR1}) - (0.25 \times \text{NIR} + 2.75 \times \text{SWIR2})$	Feyisa et al. (2014)
	Modified Normalised Difference Water Index (MNDWI)	$\frac{\text{Green} - \text{SWIR1}}{\text{Green} + \text{SWIR1}}$	Xu (2006)
	Water Ratio Index (WRI)	$\frac{\text{Green} + \text{Red}}{\text{NIR} + \text{SWIR1}}$	Shen and Li (2010)
	Normalised Difference Water Index (NDWI)	$\frac{\text{Green} - \text{NIR}}{\text{Green} + \text{NIR}}$	McFeeters (1996)
	New Water Index (NWI)	$\frac{\text{Blue} - (\text{NIR} + \text{SWIR1} + \text{SWIR2})}{\text{Blue} + (\text{NIR} + \text{SWIR1} + \text{SWIR2})}$	Ding et al. (2018)

computed in two ways, that is, first using 10m image sharpened SWIR1 or SWIR2 band(s) and secondly using 10m resampled SWIR1 or SWIR2 band(s). The intensity hue saturation (IHS) technique was adopted for sharpening the 20m low resolution SWIR1 and SWIR2 bands to 10m resolution using the 10m NIR band (Du et al., 2016). The IHS technique is one of the classical most widely used and successful image sharpening approaches which enhances the spatial resolution while maintaining the spectral fidelity of the fused image product (Du et al., 2016).

## 2.4 | Surface water and dryland reference data

Surface water availability reference data for this analysis were acquired from annual aerial survey reports which described the dry season condition of water pans during routine game counts organised by Wildlife and Environment Zimbabwe in HNP. Surface water pans which were still holding surface water in the dry season (September/October) of each year in HNP were selected. For each year an equal number of dryland sites which could be visually discerned from high-resolution imagery were selected for comparing their spectral properties with those of surface water bodies and to evaluating the capability of radar and optical methods to differentiate water bodies from dryland sites (Dzinotizei et al., 2018).

## 2.5 | Thresholding techniques

Thresholds were used for segmentation of surface water and dryland pixels. The thresholds were computed two ways, that is, using fixed optimal thresholds and automated Jenks natural breaks.

### 2.5.1 | Fixed optimal thresholds

Reference data on surface water and dryland were acquired from historical high-resolution images made available through Google Earth for April 2016 and February 2019. Sentinel-1 radar and Sentinel-2 optical images for April 2016 and February 2019 were used for surface water mapping. Thereafter, the manually iterated threshold which showed the highest agreement between ground-truth reference data and image data were selected (Vázquez-Jiménez et al., 2018). The better-performing threshold between the 2 years, that is, 2016 or 2019 was used as a fixed optimal threshold for binary classification of images for the years 2016, 2017, 2018, 2019, 2020, 2021, and 2023.

### 2.5.2 | Automated Jenks natural breaks

The Jenks natural breaks method uses an automated data clustering technique that aggregates data into two natural groupings, that is, surface water and dryland by minimising the within-group variance and maximising the between-group variance (Coulson, 1987). This automated method allows adjustment for variability in image reflectance values over time due to variations in external conditions (Du et al., 2002; Li et al., 2024). Automated Jenks natural breaks were applied to surface water and dryland data for each water detecting method for the years 2016, 2017, 2018, 2019, 2020, 2021, and 2023.

## 2.6 | Accuracy assessment

To assess the accuracy of binary image classification, a confusion matrix was generated and the overall accuracy (OA) and kappa

statistics were used to evaluate the performance of Sentinel-1 radar and Sentinel-2 optical methods for 2016–2023.

### 3 | RESULTS

#### 3.1 | Evaluating the performance of radar and optical methods using fixed optimal thresholds

The fixed optimal thresholds and corresponding OA and kappa coefficient for each water detecting method are given in Table 2. Sentinel-1 radar methods were associated with low surface water detection accuracy for the year 2016 (OA: 51%–63%) and ( $\kappa$ : 0.03–0.25). However, there was a gradual improvement in surface water detection accuracy for all Sentinel-1 radar methods from year to year. For the year 2023: VH, VV, SWI, and MSWI showed improved surface water detection accuracy (OA: 82%–91%) and ( $\kappa$ : 0.64–0.82); however, VHRVV and NDPI still performed poorly (OA: 59%–61%) and ( $\kappa$ : 0.18–0.22). At their fixed optimal thresholds, Sentinel-1 radar methods showed highly variable performance.

For all Sentinel-2 optical methods assessed there was moderate to high surface water detection accuracy for the years 2016–2021 (OA: 73%–98%) and ( $\kappa$ : 0.46–0.96). However, for the year 2023 MNDWI (sharpened), MNDWI (resampled), WRI, NDWI, and NWI showed low surface water detection accuracy (OA: 50%–76%) and ( $\kappa$ : 0.00–0.52) and only AWEI<sub>nsh</sub> (sharpened) and AWEI<sub>nsh</sub> (resampled) maintained high surface water detection accuracy (OA: 99%–100%) and ( $\kappa$ : 0.98–1.00). Based on fixed optimal thresholds, overall Sentinel-2 optical methods mostly showed consistency in performance and less temporal variability except for the year 2023. AWEI<sub>nsh</sub> (sharpened) showed the highest and most consistent surface water detection accuracy from 2016 to 2023 (OA: 94%–100%) and ( $\kappa$ : 0.88–1.00).

#### 3.2 | Evaluating the performance of radar and optical methods using automated Jenks natural breaks

The Jenk's natural break values for automated segmenting of surface water from dryland are shown in Table S1. The corresponding OA and kappa coefficient accuracy assessment measures are given in Table 3. The performance of Sentinel-1 radar methods when automated natural breaks were applied did not show much difference compared with when fixed optimal thresholds were applied.

There was an improvement in the performance of Sentinel-2 optical methods when automated natural breaks were applied for the year 2023 (Table 3), where there was a poor performance by MNDWI (sharpened), MNDWI (resampled), WRI, NDWI, and NWI when fixed optimal thresholds were applied.

#### 3.3 | Mapping surface water bodies and dryland sites using radar and optical methods

Figures S1 and S2 show maps of surface water bodies and dryland sites respectively, using Sentinel-1 radar and Sentinel-2 optical methods in a subset area of HNP for February/March 2023. Surface water body maps for radar methods show more mixed pixels compared with optical methods, which are a result of radar methods misclassifying surface water as dryland. Dryland site maps for radar VHRVV and NDPI show more mixed pixels than other radar and optical methods, which are a result of VHRVV and NDPI misclassifying dryland as surface water.

### 4 | DISCUSSION

This study showed that Sentinel-2 optical methods had higher surface water detection accuracy than Sentinel-1 radar methods. The performance of Sentinel-1 radar was highly variable over time, whereas the performance of Sentinel-2 optical methods was less variable. The performance of Sentinel-2 optical methods improved when automated natural breaks were applied instead of fixed optimal thresholds, whereas the performance of Sentinel-1 radar methods was not affected by either of the two thresholding methods.

Accuracy in the detection of surface water of variable spectral reflectance was higher with Sentinel-2 optical methods. Differences in performance may be attributed to the limited spectral information captured by Sentinel-1 radar sensor dual polarised bands and reliance on texture and homogeneity of surfaces for accurate feature detection (Kaplan & Avdan, 2018; Tamkuan & Nagai, 2021). In contrast, multispectral optical sensors may respond better to wide variations in spectral reflectance in the visible, near-infrared, and short-wave infrared regions of the electromagnetic spectra (Bioresita et al., 2019) and this is probably necessary to detect waterbodies that undergo wide variations in spectral properties in space and time (Li et al., 2022).

Surface water detection accuracy by Sentinel-1 radar methods was highly variable as shown by OA and kappa statistic assessment measures which continuously changed over time. Surface water detection for Sentinel-1 was low in year 2016 but there was a trend of gradual improvement in surface water detection each year and this resulted in high temporal variability. We speculate that this temporal variability in surface water detection could have been related to a systematic distortion in backscatter values of the Sentinel-1 images over the study region, resolved by the improvement in the technology and image quality over time. A study which monitored Tankwa non-perennial river in an arid wildlife area in South Africa using Sentinel-1 and Sentinel-2 images for the year 2016 observed low surface water detection accuracy by Sentinel-1 VV and VH bands and contrasting high surface water detection accuracy by Sentinel-2-based NDWI algorithm (Seaton & Dube, 2021). From the

TABLE 2 Accuracy assessment measures of Sentinel-1 radar and Sentinel-2 optical methods based on fixed optimal thresholds.

Sensor type	Water detecting method	Fixed optimal threshold	2016 September/October		2017 September/October		2018 September/October		2019 September/October		2020 September/October		2021 September/October		2023 February/March	
			OA (%)	Kappa	OA (%)	Kappa	OA (%)	Kappa	OA (%)	Kappa	OA (%)	Kappa	OA (%)	Kappa	OA (%)	Kappa
Sentinel-1 (radar)	VH	-22.20	59.43	0.189	65.83	0.317	66.07	0.321	72.09	0.442	67.35	0.347	77.66	0.553	85.00	0.700
	VV	-17.30	61.32	0.226	68.33	0.367	67.86	0.357	74.42	0.488	79.59	0.592	75.53	0.511	86.00	0.720
	VHVV	1.27	52.83	0.057	53.33	0.067	55.36	0.107	55.81	0.116	56.12	0.122	57.45	0.149	61.00	0.220
	NDPI	-0.13	51.89	0.038	51.67	0.033	54.46	0.089	56.98	0.140	54.08	0.082	57.45	0.149	59.00	0.180
	SWI	0.20	62.26	0.245	69.17	0.383	74.10	0.482	76.74	0.535	84.69	0.694	81.91	0.638	91.00	0.820
	MSWI	-1.70	54.72	0.094	60.00	0.200	61.61	0.232	67.44	0.349	64.29	0.286	63.83	0.277	82.00	0.640
Sentinel-2 (optical)	AWEL <sub>ns<sup>h</sup></sub> (sharpened)	-10,100	97.17	0.943	94.17	0.883	97.32	0.946	96.51	0.930	96.94	0.939	97.87	0.957	100.00	1.000
	AWEL <sub>ns<sup>h</sup></sub> (resampled)	-9600	75.47	0.509	88.33	0.767	85.71	0.714	73.26	0.465	85.71	0.714	92.55	0.851	99.00	0.980
	MNDWI (sharpened)	-0.35	82.08	0.642	80.83	0.617	96.43	0.929	89.53	0.791	92.86	0.857	95.74	0.915	76.00	0.520
	MNDWI (resampled)	-0.39	81.13	0.623	89.17	0.783	91.07	0.821	80.23	0.605	80.61	0.612	94.68	0.894	50.00	0.000
	WRI	0.49	83.96	0.679	85.83	0.717	90.18	0.804	90.70	0.814	90.82	0.816	92.55	0.851	71.00	0.420
	NDWI	-0.35	82.08	0.642	80.83	0.617	96.43	0.929	89.53	0.791	92.86	0.857	95.74	0.915	74.00	0.480
NWI	-0.80	91.51	0.830	95.00	0.900	93.75	0.875	89.53	0.791	86.74	0.735	94.68	0.894	50.00	0.000	

Abbreviation: OA, overall accuracy.

TABLE 3 Accuracy assessment measures of Sentinel-1 radar and Sentinel-2 optical methods based on automated Jenks natural breaks.

Sensor type	Water detecting method	2016 September/October		2017 September/October		2018 September/October		2019 September/October		2020 September/October		2021 September/October		2023 February/March	
		OA (%)	Kappa	OA (%)	Kappa	OA (%)	Kappa	OA (%)	Kappa	OA (%)	Kappa	OA (%)	Kappa	OA (%)	Kappa
Sentinel-1 (radar)	VH	59.43	0.189	64.17	0.283	67.86	0.357	73.26	0.465	61.22	0.224	72.34	0.447	81.00	0.620
	VV	52.83	0.057	57.50	0.150	66.96	0.339	67.44	0.349	64.29	0.286	75.53	0.510	88.00	0.760
	VH+VV	50.00	0.000	50.00	0.000	50.00	0.000	50.00	0.000	50.00	0.000	51.06	0.021	53.00	0.060
	NDPI	50.94	0.019	50.00	0.000	51.79	0.036	50.00	0.000	54.08	0.082	52.13	0.043	55.00	0.100
	SWI	66.04	0.321	70.83	0.417	81.25	0.625	80.23	0.605	82.65	0.653	88.30	0.766	87.00	0.740
	MSWI	63.21	0.264	65.83	0.317	65.18	0.304	70.93	0.419	68.37	0.367	73.40	0.468	83.00	0.660
Sentinel-2 (optical)	AWEI <sub>nsh</sub> (sharpened)	98.11	0.962	95.00	0.900	100.00	1.000	97.67	0.953	95.92	0.918	100.00	1.000	99.00	0.980
	AWEI <sub>nsh</sub> (resampled)	87.74	0.755	91.67	0.833	89.29	0.786	90.70	0.814	81.63	0.633	97.87	0.957	96.00	0.920
	MNDWI (sharpened)	93.40	0.868	84.17	0.683	82.14	0.643	93.02	0.860	97.96	0.959	90.43	0.809	87.00	0.740
	MNDWI (resampled)	74.53	0.491	85.00	0.700	84.82	0.696	73.26	0.465	65.31	0.306	82.98	0.660	89.00	0.780
	WRI	77.36	0.547	77.50	0.550	80.36	0.607	72.09	0.442	66.33	0.327	79.79	0.596	87.00	0.740
	NDWI	97.17	0.943	97.50	0.950	94.64	0.893	94.19	0.884	95.92	0.918	100.00	1.000	98.00	0.960
	NWI	76.42	0.528	82.50	0.650	83.93	0.679	75.58	0.512	66.33	0.327	84.04	0.681	91.00	0.820

Abbreviation: OA, overall accuracy.

long-term evaluation done in this study, it can be acknowledged that surface detection by all Sentinel-1 radar methods was initially low but notably improved over time.

Overall, the multiband optical AWEI<sub>nsh</sub> (sharpened) had the highest surface water detection accuracy compared with all other spectral band combination methods. The optical AWEI<sub>nsh</sub> (sharpened) proved to be robust to spectral complexities of surface water bodies in the heterogeneous semi-arid protected area. This might be attributed to the incorporated SWIR bands in the algorithm, which are robust to spectral variability of surface water and less responsive to concentrations of sediments and other optically active constituents (Huang et al., 2018; Yang & Chen, 2017). Fusing the SWIR bands with the NIR band yielded better results compared with using SWIR bands alone because of the sensitivity of the NIR band to chlorophyll-*a* constituents, for example, in phytoplankton (Kutser, 2009) and the spectral contrast between surface water and land, enabling high surface water detection accuracy (Mondegar & Tongco, 2019).

The performance of Sentinel-2 optical methods can be optimised using automated natural breaks. For the year 2023, Sentinel-2 optical MNDWI (resampled) and NWI calculated using fixed optimal thresholds, failed to accurately detect surface water. When automated natural breaks were applied, surface water detection markedly improved. Of exception is the optical AWEI<sub>nsh</sub> (sharpened) whose surface water detection accuracy was consistent regardless of the thresholding method applied. The stability of thresholds can be explained by the integrated coefficients in the AWEI algorithm intended to minimise spectral overlap between diverse land cover classes, allowing them to be easily segmented by thresholds (Feyisa et al., 2014; Zhai et al., 2015).

In the absence of ground reference data for automated image-scene-based thresholding, the stable and robust AWEI<sub>nsh</sub> (sharpened) can be applied using fixed-optimal thresholds. Where optical-based technologies are impeded as a result of radiation scattering by tree canopies and clouds, especially during the wet season in semi-arid Savanna ecosystems, there is a need to continually explore robust radar methods because they allow regular surface water monitoring. Other techniques which can improve the performance of Sentinel-1 radar methods, for example, texture and geometry metrics and machine and deep learning models need to be explored for optimal detection of surface water of high-spectral variability using radar imagery in semi-arid protected areas.

#### FUNDING INFORMATION

No funders available.

#### CONFLICT OF INTEREST STATEMENT

No potential conflict of interest was reported by the author(s).

#### DATA AVAILABILITY STATEMENT

The data that support the findings of this study are available from the corresponding author upon reasonable request.

#### ORCID

Hilton G. T. Ndagurwa  <https://orcid.org/0000-0002-9349-6548>

Henry Ndaimani  <https://orcid.org/0000-0002-8237-8140>

#### REFERENCES

- Bartzke, G. S., Ogotu, J. O., Mukhopadhyay, S., Mtui, D., Dublin, H. T., & Piepho, H. P. (2018). Rainfall trends and variation in the Maasai Mara ecosystem and their implications for animal population and biodiversity dynamics. *PLoS One*, 13(9), e0202814. <https://doi.org/10.1371/journal.pone.0202814>
- Behnamian, A., Banks, S., White, L., Brisco, B., Millard, K., Pasher, J., Chen, Z., Duffe, J., Bourgeau-Chavez, L., & Battaglia, M. (2017). Semi-automated surface water detection with synthetic aperture radar data: A wetland case study. *Remote Sensing*, 9(12), 1209. <https://doi.org/10.3390/rs9121209>
- Bhangale, U., More, S., Shaikh, T., Patil, S., & More, N. (2020). Analysis of surface water resources using Sentinel-2 imagery. *Procedia Computer Science*, 171, 2645–2654. <https://doi.org/10.1016/j.procs.2020.04.287>
- Bioresita, F., Puissant, A., Stumpf, A., & Malet, J. P. (2019). Fusion of Sentinel-1 and Sentinel-2 image time series for permanent and temporary surface water mapping. *International Journal of Remote Sensing*, 40(23), 9026–9049. <https://doi.org/10.1080/01431161.2019.1624869>
- Brisco, B. (2015). Mapping and monitoring surface water and wetlands with synthetic aperture radar. In R. W. Tiner, M. W. Lang, & V. V. Klemas (Eds.), *Remote sensing of wetlands: Applications and advances* (pp. 119–136). CRC Press.
- Chamaillé-Jammes, S., Valeix, M., & Fritz, H. (2007). Managing heterogeneity in elephant distribution: Interactions between elephant population density and surface-water availability. *Journal of Applied Ecology*, 44(3), 625–633. <https://doi.org/10.1111/j.1365-2664.2007.01300.x>
- Clement, M. A., Kilsby, C. G., & Moore, P. (2018). Multi-temporal synthetic aperture radar flood mapping using change detection. *Journal of Flood Risk Management*, 11(2), 152–168. <https://doi.org/10.1111/jfr3.12303>
- Coulson, M. R. C. (1987). In the matter of class intervals for choropleth maps: With particular reference to the work of George F Jenks. *Cartographica: The International Journal for Geographic Information and Geovisualization*, 24, 16–39. <https://doi.org/10.3138/U7X0-1836-5715-3546>
- Davidson, Z., Valeix, M., Van Kesteren, F., Loveridge, A. J., Hunt, J. E., Murindagomo, F., & Macdonald, D. W. (2013). Seasonal diet and prey preference of the African lion in a waterhole-driven semi-arid savanna. *PLoS One*, 8, e55182. <https://doi.org/10.1371/journal.pone.0055182>
- Ding, J., Cuo, L., Zhang, Y., & Zhu, F. (2018). Monthly and annual temperature extremes and their changes on the Tibetan Plateau and its surroundings during 1963–2015. *Scientific Reports*, 8(1), 1–23. <https://doi.org/10.1038/s41598-018-30320-0>
- Du, Y., Teillet, P. M., & Cihlar, J. (2002). Radiometric normalization of multitemporal high-resolution satellite images with quality control for land cover change detection. *Remote Sensing of Environment*, 82(1), 123–134. [https://doi.org/10.1016/S0034-4257\(02\)00029-9](https://doi.org/10.1016/S0034-4257(02)00029-9)
- Du, Y., Zhang, Y., Ling, F., Wang, Q., Li, W., & Li, X. (2016). Water bodies' mapping from Sentinel-2 imagery with modified normalized difference water index at 10-m spatial resolution produced by sharpening the SWIR band. *Remote Sensing*, 8(4), 354. <https://doi.org/10.3390/rs8040354>
- Dzinotizei, Z., Murwira, A., Zengeya, F. M., & Guerrini, L. (2018). Mapping waterholes and testing for aridity using a remote sensing water index in a southern African semi-arid wildlife area. *Geocarto*

- International*, 33(11), 1268–1280. <https://doi.org/10.1080/10106049.2017.1343394>
- ESA. (2020). ESA Sen2Cor v2.5.5. [https://step.esa.int/main/snap-support-ed-plugins/sen2cor/sen2cor\\_v2-5-5/](https://step.esa.int/main/snap-support-ed-plugins/sen2cor/sen2cor_v2-5-5/)
- Feyisa, G. L., Meilby, H., Fensholt, R., & Proud, S. R. (2014). Automated Water Extraction Index: A new technique for surface water mapping using Landsat imagery. *Remote Sensing of Environment*, 140, 23–35. <https://doi.org/10.1016/j.rse.2013.08.029>
- Filipponi, F. (2019). Sentinel-1 GRD preprocessing workflow. *Multidisciplinary Digital Publishing Institute Proceedings*, 18(1), 11. <https://doi.org/10.3390/ECRS-3-06201>
- Gangat, R., Van Deventer, H., Naidoo, L., & Adam, E. (2020). Estimating soil moisture using Sentinel-1 and Sentinel-2 sensors for dryland and palustrine wetland areas. *South African Journal of Science*, 116(7–8), 1–9. <https://doi.org/10.17159/sajs.2020/6535>
- Gaylard, A., Owen-Smith, N., & Redfern, J. (2003). Surface water availability: Implications for heterogeneity and ecosystem processes. In T. Du Toit, K. H. Rogers, & H. C. Biggs (Eds.), *The Kruger experience: Ecology and management of savanna heterogeneity* (pp. 171–188). Island Press.
- Gupta, R. P. (2017). *Remote sensing geology*. Springer Verlag.
- Huang, C., Nguyen, B. D., Zhang, S., Cao, S., & Wagner, W. (2017). A comparison of terrain indices toward their ability in assisting surface water mapping from Sentinel-1 data. *ISPRS International Journal of Geo-Information*, 6(5), 140. <https://doi.org/10.3390/ijgi6050140>
- Huang, W., DeVries, B., Huang, C., Lang, M. W., Jones, J. W., Creed, I. F., & Carroll, M. L. (2018). Automated extraction of surface water extent from Sentinel-1 data. *Remote Sensing*, 10(5), 797. <https://doi.org/10.3390/rs10050797>
- Kaplan, G., & Avdan, U. (2017). Mapping and monitoring wetlands using Sentinel-2 satellite imagery. *ISPRS Annals of the Photogrammetry, Remote Sensing and Spatial Information Sciences*, 4, 271–277. <https://doi.org/10.5194/isprs-annals-IV-4-W4-271-2017>
- Kaplan, G., & Avdan, U. (2018). Sentinel-1 and Sentinel-2 data fusion for wetlands mapping: Balıkdami, Turkey. *The International Archives of the Photogrammetry, Remote Sensing and Spatial Information Sciences*, 42, 729–734. <https://doi.org/10.5194/isprs-archives-XLII-3-729-2018>
- Kim, Y., & Van Zyl, J. J. (2009). A time-series approach to estimate soil moisture using polarimetric radar data. *IEEE Transactions on Geoscience and Remote Sensing*, 47(8), 2519–2527. <https://doi.org/10.3390/rs12182919>
- Kutser, T. (2009). Passive optical remote sensing of cyanobacteria and other intense phytoplankton blooms in coastal and inland waters. *International Journal of Remote Sensing*, 30(17), 4401–4425. <https://doi.org/10.1080/01431160802562305>
- Li, J., Ma, R., Cao, Z., Xue, K., Xiong, J., Hu, M., & Feng, X. (2022). Satellite detection of surface water extent: A review of methodology. *Water*, 14(7), 1148. <https://doi.org/10.3390/w14071148>
- Li, L., Jiang, Y., Shen, X., & Li, D. (2024). Long-term assessment and analysis of the radiometric quality of standard data products for Chinese Gaofen-1/2/6/7 optical remote sensing satellites. *Remote Sensing of Environment*, 308, 114169. <https://doi.org/10.1016/j.rse.2024.114169>
- Markert, K. N., Chishtie, F., Anderson, E. R., Saah, D., & Griffin, R. E. (2018). On the merging of optical and SAR satellite imagery for surface water mapping applications. *Results in Physics*, 9, 275–277. <https://doi.org/10.1016/j.rinp.2018.02.054>
- McFeeters, S. K. (1996). The use of the normalized difference water index (NDWI) in the delineation of open water features. *International Journal of Remote Sensing*, 17(7), 1425–1432. <https://doi.org/10.1080/01431169608948714>
- Mishra, V., Limaye, A. S., Muench, R. E., Cherrington, E. A., & Markert, K. N. (2020). Evaluating the performance of high-resolution satellite imagery in detecting ephemeral water bodies over West Africa. *International Journal of Applied Earth Observation and Geoinformation*, 93, 102218. <https://doi.org/10.1016/j.jag.2020.102218>
- Mitchard, E. T., Saatchi, S. S., White, L. J., Abernethy, K. A., Jeffery, K. J., Lewis, S. L., Collins, M., Lefsky, M. A., Leal, M. E., Woodhouse, I. H., & Meir, P. (2012). Mapping tropical forest biomass with radar and spaceborne LiDAR in Lopé National Park, Gabon: Overcoming problems of high biomass and persistent cloud. *Biogeosciences*, 9(1), 179–191. <https://doi.org/10.5194/bg-9-179-2012>
- Mondegar, J. P., & Tongco, A. F. (2019). Near infrared band of Landsat 8 as water index: A case study around Cordova and Lapu-Lapu City, Cebu, Philippines. *Sustainable Environment Research*, 29(16), 1–15. <https://doi.org/10.1186/s42834-019-0016-5>
- Ovakoglou, G., Cherif, I., Alexandridis, T. K., Pantazi, X. E., Tamouridou, A. A., Moshou, D., Tseni, X., Raptis, I., Kalaitzopoulou, S., & Mourelatos, S. (2021). Automatic detection of surface-water bodies from Sentinel-1 images for effective mosquito larvae control. *Journal of Applied Remote Sensing*, 15(1), 14507. <https://doi.org/10.1117/1.JRS.15.014507>
- Owen-Smith, N. (1996). Ecological guidelines for waterpoints in extensive protected areas. *South African Journal of Wildlife Research-24-Month Delayed Open Access*, 26(4), 107–112.
- Peña-Luque, S., Ferrant, S., Cordeiro, M. C. R., Ledauphin, T., Maxant, J., & Martinez, J. M. (2021). Sentinel-1&2 multitemporal water surface detection accuracies, evaluated at regional and reservoirs level. *Remote Sensing*, 13(16), 3279. <https://doi.org/10.3390/rs13163279>
- Rogers, C. (1993). Woody vegetation survey of Hwange National Park: A report prepared for the Department of National Parks and Wild Life Management, Zimbabwe. Department of National Parks and Wild Life Management. En Plant records. Geog 5. 176p.-illus.
- Rotkiske, T. A., & Bostater, C. R., Jr. (2018). Influence of bottom depths and bottom types on water surface reflectance. Remote sensing of the ocean, sea ice, coastal waters, and large water regions. *Proceedings of SPIE*, 10784, B1–B11. <https://doi.org/10.1117/12.2515669>
- Seaton, D., & Dube, T. (2021). A new modified spatial approach for monitoring non-perennial river water availability using remote sensing in the Tankwa Karoo, Western Cape, South Africa. *Water SA*, 47(3), 338–346. <https://doi.org/10.17159/wsa/2021.v47.i3.11862>
- Senay, G. B., Velpuri, N. M., Alemu, H., Pervez, S. M., Asante, K. O., Kariuki, G., Taa, A., & Angerer, J. (2013). Establishing an operational waterhole monitoring system using satellite data and hydrologic modelling: Application in the pastoral regions of East Africa. *Pastoralism: Research, Policy and Practice*, 3, 20. <https://doi.org/10.1186/2041-7136-3-20>
- Shen, L., & Li, C. (2010). Water body extraction from Landsat ETM+ imagery using adaboost algorithm. In 2010 18th International Conference on Geoinformatics, Beijing, June 1–4 <https://doi.org/10.1109/GEOINFORMATICS.2010.5567762>
- Slagter, B., Tsendbazar, N. E., Vollrath, A., & Reiche, J. (2020). Mapping wetland characteristics using temporally dense Sentinel-1 and Sentinel-2 data: A case study in the St. Lucia wetlands, South Africa. *International Journal of Applied Earth Observation and Geoinformation*, 86, 102009. <https://doi.org/10.1016/j.jag.2019.102009>
- Smit, I. P., Grant, C. C., & Devereux, B. J. (2007). Do artificial waterholes influence the way herbivores use the landscape? Herbivore distribution patterns around rivers and artificial surface water sources in a large African savanna park. *Biological Conservation*, 136(1), 85–99. <https://doi.org/10.1016/j.biocon.2006.11.009>
- Tamkuan, N., & Nagai, M. (2021). ALOS-2 and Sentinel-1 backscattering coefficients for water and flood detection in Nakhon Phanom Province, northeastern Thailand. *International Journal of Geoinformatics*, 17(3), 39–48. <https://doi.org/10.52939/ijg.v17i3.1895>
- Tian, H., Li, W., Wu, M., Huang, N., Li, G., Li, X., & Niu, Z. (2017). Dynamic monitoring of the largest freshwater lake in China using a new water index derived from high spatiotemporal resolution sentinel-1A data. *Remote Sensing*, 9(6), 521. <https://doi.org/10.3390/rs9060521>

- Vázquez-Jiménez, R., Ramos-Bernal, R. N., Romero-Calcerrada, R., Arrogante-Funes, P., Tizapa, S. S., & Novillo, C. J. (2018). Thresholding algorithm optimization for change detection to satellite imagery. In C. M. Travieso-Gonzalez (Ed.), *Colorimetry and image processing* (pp. 163–182). Intech Open. <https://doi.org/10.5772/intechopen.71002>
- Wang, J., Ding, J., Li, G., Liang, J., Yu, D., Aishan, T., Zhang, F., Yang, J., Abulimiti, A., & Liu, J. (2019). Dynamic detection of water surface area of Ebinur Lake using multi-source satellite data (Landsat and sentinel-1A) and its responses to changing environment. *Catena*, 177, 189–201. <https://doi.org/10.1016/j.catena.2019.02.020>
- Xu, H. (2006). Modification of normalised difference water index (NDWI) to enhance open water features in remotely sensed imagery. *International Journal of Remote Sensing*, 27(14), 3025–3033. <https://doi.org/10.1080/01431160600589179>
- Yang, X., & Chen, L. (2017). Evaluation of automated urban surface water extraction from sentinel-2A imagery using different water indices. *Journal of Applied Remote Sensing*, 11(2), 026016. <https://doi.org/10.1117/1.JRS.11.026016>
- Zeng, L., Schmitt, M., Li, L., & Zhu, X. X. (2017). Analysing changes of the Poyang Lake water area using Sentinel-1 synthetic aperture radar imagery. *International Journal of Remote Sensing*, 38(23), 7041–7069. <https://doi.org/10.1080/01431161.2017.1370151>
- Zhai, K., Wu, X., Qin, Y., & Du, P. (2015). Comparison of surface water extraction performances of different classic water indices using OLI and TM imageries in different situations. *Geospatial Information Science*, 18(1), 32–42. <https://doi.org/10.1080/10095020.2015.1017911>

## SUPPORTING INFORMATION

Additional supporting information can be found online in the Supporting Information section at the end of this article.

**How to cite this article:** Dzinotizei, Z., Ndagurwa, H. G. T., Ndaimani, H., & Chichinye, A. (2024). Comparability of radar and optical methods in identifying surface water in a semi-arid protected area. *African Journal of Ecology*, 62, e13301. <https://doi.org/10.1111/aje.13301>